A structural glaciological analysis of the 2002 Larsen B ice shelf collapse

N.F. GLASSER,[1] T.A. SCAMBOS[2]

[1]*Centre for Glaciology, Institute of Geography and Earth Sciences, Aberystwyth University, Aberystwyth SY23 3DB, UK*
E-mail: nfg@aber.ac.uk
[2]*National Snow and Ice Data Center, CIRES, University of Colorado, Boulder, Colorado 80309-0449, USA*

ABSTRACT. This study provides a detailed structural glaciological analysis of changes in surface structures on the Larsen B ice shelf on the Antarctic Peninsula prior to its collapse in February–March 2002. Mapped features include the ice-shelf front, rifts, crevasses, longitudinal linear surface structures and meltwater features. We define domains on the ice shelf related to glacier source areas and demonstrate that, prior to collapse, the central Larsen B ice shelf consisted of four sutured flow units fed by Crane, Jorum, Punchbowl and Hektoria/Green/Evans glaciers. Between these flow units were 'suture zones' of thinner ice where the feeder glaciers merged. Prior to collapse, large open-rift systems were present offshore of Foyn Point and Cape Disappointment. These rifts became more pronounced in the years preceding break-up, and ice blocks in the rifts rotated because of the strong lateral shear in this zone. Velocity mapping of the suture zones indicates that the major rifts were not present more than about 20 years ago. We suggest that the ice shelf was preconditioned to collapse by partial rupturing of the sutures between flow units. This, we believe, was the result of ice-shelf front retreat during 1998–2000, reducing the lateral resistive stress on the upstream parts of the shelf and glacier flow units, ice-shelf thinning and pre-shelf-break-up glacier acceleration.

INTRODUCTION

Ice shelves fringe ~45% of the Antarctic continent. They are important in global Earth-system processes for five main reasons: (1) ice shelves play a significant role in the global ice-volume/sea-level system because the calving of icebergs from their termini accounts for ~90% of Antarctic ice loss (Vaughan and Doake, 1996; MacAyeal and others, 2003); (2) ice shelves influence the dynamics, and therefore the system response time, of upstream inland Antarctic ice (Rott and others, 2002; De Angelis and Skvarca, 2003; Scambos and others, 2004); (3) rapid heat exchange in sub-ice-shelf cavities has a significant impact on the global ocean heat budget (Williams and others, 2001; Joughin and Padman, 2003); (4) ice shelves are capable of entraining, transporting and depositing large quantities of glacigenic material (Evans and Pudsey, 2002; Evans and Ó Cofaigh, 2003; Glasser and others, 2006); and (5) catastrophic iceberg-calving events from ice shelves have been proposed as a cause of major Late Quaternary climatic perturbations (Hulbe and others, 2004).

Ice-shelf collapse and regrowth has occurred in the recent geological past. The sedimentary record on the continental shelf indicates that some Antarctic Peninsula ice shelves (e.g. the Prince Gustav Channel Ice Shelf (Pudsey and Evans, 2001) and the George VI Ice Shelf (Hjort and others, 2001)) retreated in the mid-Holocene and may follow an asymmetrical cyclic process, involving rapid disintegration followed by gradual expansion. However, the collapse of the Larsen B ice shelf is apparently unprecedented in the Holocene (Domack and others, 2005). Recent mass loss from the northern Antarctic Peninsula is estimated to be sufficient to raise eustatic sea level by between 0.1 (Rignot and others, 2005) and $0.16 \pm 0.06\,\mathrm{mm\,a^{-1}}$ (Pritchard and Vaughan, 2007).

Most of the ice shelves that have retreated on the Antarctic Peninsula have shown two phases of retreat: a climatically driven progressive retreat that occurred for years (and in some cases decades) and a more rapid collapse phase (Doake and others, 1998; MacAyeal and others, 2003; Morris and Vaughan, 2003; Scambos and others, 2003; Vieli and others, 2006, 2007). There are indications that, in some cases, ice-shelf collapse events are a direct result of recent atmospheric or oceanic warming (Rott and others, 1998; Scambos and others, 2000; Shepherd and others, 2003). The limit for ice-shelf viability coincides with the –1.5°C January isotherm and the –5°C mean annual isotherm, both of which have moved further south during the last 50 years (Rott and others, 1996, 1998; Vaughan and Doake, 1996; Morris and Vaughan, 2003). Because mean summer temperatures have risen to near-melting and the length of the melt season has doubled during the last two decades, meltwater ponds have appeared on the surface of many Antarctic Peninsula ice shelves during the melt season (Van den Broeke, 2005). It has been suggested that this meltwater acts as a mechanical force in the crevasses, causing breaks in the ice shelf and thus accelerating ice-shelf disintegration (MacAyeal and others, 2003; Scambos and others, 2003; Van der Veen, 2007).

Here we present the results of detailed structural mapping of the Larsen B ice shelf and its tributary glaciers in the period just preceding and immediately after the 2002 ice-shelf collapse. The Larsen Ice Shelf was first given the sub-names Larsen ice shelf A, B, C and D by Vaughan and Doake (1996) (Fig. 1). Of these ice shelves only the southwest corner of the Larsen B, and the Larsen C and D remain. Larsen A ice shelf collapsed in January 1995 with the loss of $1600\,\mathrm{km^2}$ of ice shelf (Rott and others, 1996). Larsen B partially collapsed in February–March 2002 with the loss of $3200\,\mathrm{km^2}$ of ice shelf (Scambos and others, 2003; Rack and Rott, 2004). There are existing descriptions of the surface features of Antarctic ice shelves (e.g. Crabtree and Doake, 1980; Reynolds and Hambrey, 1988; Swithinbank and

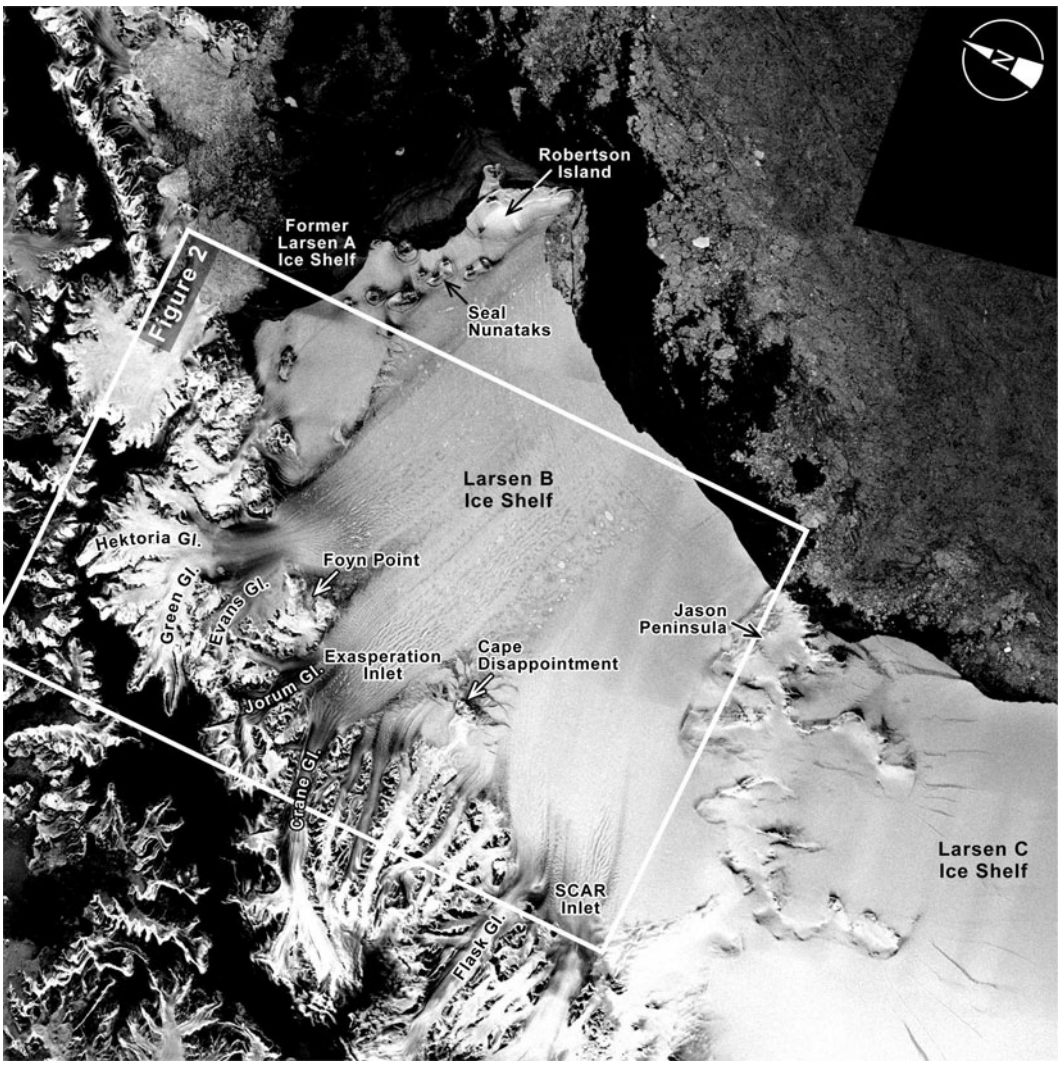

Fig. 1. Portion of the 1997 RAMP (RADARSAT-1 Antarctic Mapping Project) mosaic showing the Antarctic Peninsula and place names mentioned in the text. The location of the mapped area shown in Figure 2 is indicated.

others, 1988; Casassa and Brecher, 1993; Hambrey and Dowdeswell, 1994; Skvarca, 1994; Bindschadler and others, 2002; Evans and Ó Cofaigh, 2003), but very little is known about the temporal changes in these surface features and the role that they play in ice-shelf break-up.

METHODS

Surface structures in the Larsen B ice shelf area and its tributary glaciers were mapped from satellite imagery in ArcMap GIS (Geographical Information System) software using time-separated images. We undertook detailed studies of the ice shelf using Landsat 7 ETM+ (Enhanced Thematic Mapper Plus) and ASTER (Advanced Spaceborne Thermal Emission and Reflection Radiometer) scenes obtained before, during and after ice-shelf collapse. Image acquisition dates used in this study are: three ASTER granules acquired on 22 November 2001, and Landsat 7 scenes acquired on 27 January 2000, 21 February 2000, 6 December 2001 and 6 April 2002 (Table 1). Features mapped include the location

Table 1. Details of satellite images used in this study

Date	Sensor	Scene ID	Centre
22 Nov 2001	ASTER	AST_L1B00311222001131915	64°50′22.67″ S, 61°16′43.48″ W
22 Nov 2001	ASTER	AST_L1B00311222001131933	65°50′26.43″ S, 62°18′3.44″ W
22 Nov 2001	ASTER	AST_L1B00311222001131924	65°20′49.59″ S, 61°44′42.77″ W
27 Jan 2000	Landsat 7	LE7217106000002750	65°24′29.19″ S, 61°4′18.56″ W
21 Feb 2000	Landsat 7	L71216106_10620000221	65°23′33.84″ S, 61°3′58.90″ W
6 Dec 2001	Landsat 7	LE7218106000134050	65°39′59.13″ S, 62°46′55.46″ W
6 Apr 2002	Landsat 7	LE7217106000209650	65°32′48.05″ S, 61°19′13.96″ W

Table 2. Features mapped on the satellite images, together with their identification criteria and possible significance

Feature	Identification on satellite imagery	Significance
Ice-shelf edge	Abrupt transition from ice shelf to ocean. Calved icebergs often visible in ocean in front of the ice shelf.	Indicates maximum extent of the ice shelf. Time series can be used to trace advance or recession of ice-shelf extent through time.
Rifts	Surface crack with a visible opening, usually oriented at right angles to the flow direction and deep enough to penetrate the ice-shelf thickness.	Rifts are formed when the stresses within the ice exceed a temperature-dependent threshold. Formed perpendicular to the direction of maximum tension.
Crevasses and crevasse fields	Surface cracks appearing either as white lines (snow-filled) or dark lines (non-snow-filled or water-filled), which cross-cut other features. Varied orientation with respect to ice flow.	Crevasses are formed when the stresses within the ice exceed a temperature-dependent threshold. Formed perpendicular to the direction of maximum tension. Open crevasses may indicate locations of extensional flow.
Longitudinal surface structures (also known as flow stripes, flowbands, flowlines, streak lines or foliation)	Long linear pervasive layered structure parallel to ice movement. Horizontal dimensions of 1 km or less but can extend for many tens or even hundreds of kilometres. Often generated in regions of positive relief, at bed protuberances or in regions of increased basal friction. Often seen to emanate from the confluences of separate ice streams or glaciers.	Provides visual impression of the direction of ice motion. Cumulative length is due to slow decay timescale relative to the time required for ice to travel a long distance.
Flow-unit boundary	Structural discontinuity or junction that separates structures rotated in one orientation from structures rotated in a different orientation. Structures may be 'smeared' along the junction.	Indicates confluence of individual flow units or glaciers.
Transverse/arcuate structures	Straight dark lines in areas of crevassing. Can be followed down-glacier as deforming dark lines, often turning into arcuate structures and cross-cutting previously formed structures.	Crevasse traces, indicating incipient or closed crevasses.
Grounding line	Appears as abrupt break in surface slope or area of intense crevassing. Meltwater ponds may form preferentially at the grounding line if there is a change in gradient across the grounding line.	Junction between grounded and floating ice.
Folds and fold structures	Large-scale folding appears as bends or curves in otherwise linear features which do not follow surface topography.	Indicates presence of folding, usually under compressive regime.
Ice rises	Elevation of ice surface, with disturbance to ice flow indicated by smooth surface and associated crevasses in the lee of the ice rise.	Indicates area where ice shelf is grounded on local bedrock high.
Ice rumples	Elevation of ice surface, with disturbance to ice flow indicated by crevasses. Ice flow continues across basal high.	Indicates area where ice shelf is grounded on local bedrock high.
Surface debris	Accumulations of surface material indicated by lines or bands of debris. Often orientated parallel to flow (i.e. along longitudinal foliation).	Provides visual impression of the ice-motion direction and magnitude where redistributed by ice flow.
Meltwater ponds, streams, dolines, drained lakes	Dark, flat areas on ice-shelf surface. May or may not form along pre-existing structural discontinuities.	Indicates significant surface ablation. Dolines and drained lakes may indicate a connection between ice-shelf surface and subsurface

of the ice-shelf front, the location of rifts (fractures that penetrate the entire ice-shelf thickness), longitudinal surface structures (also known as flow stripes or streak lines), individual flow units, medial moraines and other areas of surface debris, open crevasses and surface meltwater features (streams, ponds, meltwater-filled crevasses and dolines). A complete list of mapped features, with their identification criteria and significance, is provided in Table 2. Satellite image interpretation was performed using multiple band combinations and standard image enhancement procedures (contrast stretching and histogram equalization) to improve the contrast across features. The horizontal resolution of the satellite images (15 m for both the Landsat 7 ETM+ band 8 images and the ASTER band 3N images) is a limitation on the minimum size of the features mapped. Detailed mapping was carried out by hand-digitizing features in ArcMap at 1 : 50 000 scale.

RESULTS

The results of the mapping are presented below in five parts. We consider (1) ice-shelf tributary-glacier domains on the surface of the ice shelf, (2) meltwater-pond and drainage patterns on the shelf, (3) large-scale changes in the Larsen B ice shelf between January 2000 and April 2002, (4) changes in the tributary-glacier rift systems between February 2000 and April 2002 and (5) changes in ice-shelf tributary glaciers between February 2000 and April 2002. Interpretations of the glaciological significance of the mapped features are presented separately.

Ice-shelf tributary-glacier domains

In the November 2001 ASTER satellite images, the Larsen B ice shelf is composed of at least 14 individual glacier domains (marked as domains 3–16 in Fig. 2). Domains 1

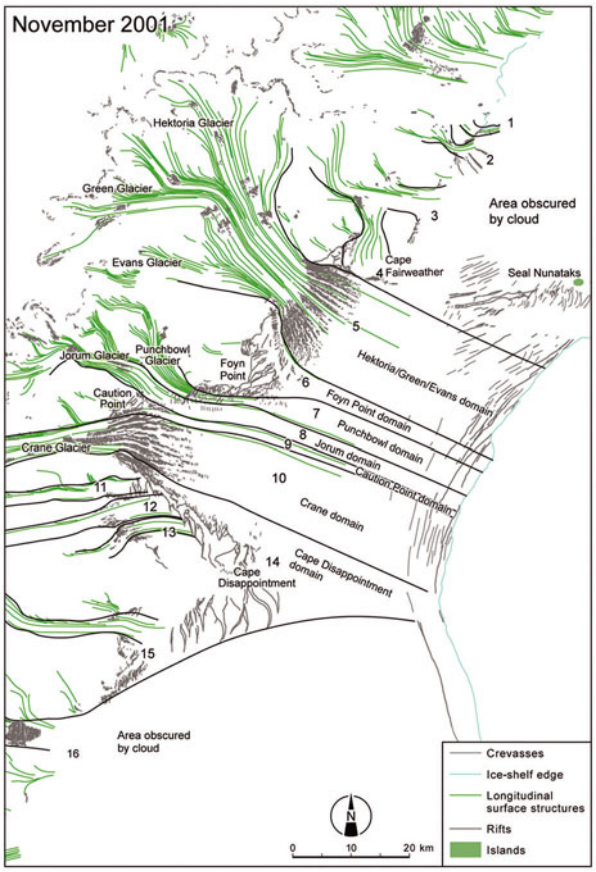

Fig. 2. Tributary-glacier domains on the former Larsen B ice shelf inferred from crevasse patterns and longitudinal surface structures on ASTER mosaic in November 2001. Numbers refer to domains discussed in the text.

and 2 contribute ice to the former Larsen A ice shelf and domains 3 and 4 contribute little ice volume to the Larsen B ice shelf so are not discussed in detail here. By far the largest contribution to the disintegrated portion of the former Larsen B ice shelf comes from four tributary glaciers: the Hektoria/Green/Evans glacier system (domain 5 in Fig. 2), Punchbowl Glacier (domain 7 in Fig. 2), Jorum Glacier (domain 8 in Fig. 2) and Crane Glacier (domain 10 in Fig. 2). These glaciers feed the ice shelf from narrow glacial valleys, and the glacier ice spreads laterally just downstream of their grounding lines. Splaying crevasse patterns and transverse separation of longitudinal surface structures mark this zone (Fig. 2).

Longitudinal surface structures originating in the trunks of these glaciers can be traced uninterrupted all the way to the ice-shelf front. Four smaller tributary glaciers (domains 11–13 and 15) also flow towards the ice shelf but do not contribute significantly to its downstream surface area (Fig. 2). These glaciers are separated from the ice shelf by a large rift originating at the southern end of the grounding line for Crane Glacier and extending out to and past Cape Disappointment. Between domains 5 and 7, 8 and 10, and 10 and 16 are domains lacking significant up-glacier catchments and without longitudinal surface structures (domain 6 originating from Foyn Point, domain 9 originating from Caution Point and domain 14 originating from Cape Disappointment; Fig. 2). Large rift systems are also present on the ice-shelf surface at Foyn Point and Cape Disappointment.

Individual glacier domains on the ice shelf possess very different surface characteristics. The Hektoria/Green/Evans domain (domain 5 in Fig. 2) has both surface meltwater ponds and streams (Fig. 3a), whilst the Crane domain (domain 10 in Fig. 2) has a much rougher, 'pockmarked' surface texture consisting of elongate depressions (some of which are meltwater-filled lakes in summer) separated by ridges.

Meltwater-pond and drainage patterns on the shelf

By the austral summer of 2000, the northern and central parts of the Larsen B ice shelf had developed an extensive pattern of meltwater ponds and drainage systems. This was the culmination of a steady increase in the extent of meltwater features and the frequency of warm summers that led to extensive surface melt (MacAyeal and others, 2003; Scambos and others, 2003; Van den Broeke, 2005).

Surface meltwater features dominate the surface of Larsen B ice shelf in both January 2000 (Fig. 3a) and February 2000 (Fig. 3b). Three zones (labelled 1–3 in Fig. 3b) can be clearly distinguished: (1) a zone dominated by linear meltwater features on the northern part of the ice shelf, sometimes forming sinuous drainage networks; (2) a complex system of meltwater features in the area of the ice shelf dominated by the inflow of the Hektoria/Green/Evans glacier system, Jorum Glacier and Crane Glacier where meltwater ponds and streams appear to follow the local topographic slope on the ice-shelf surface (upper part of the image) and fill depressions on its surface along longitudinal surface structures (centre of the image); and (3) an area almost devoid of surface meltwater features on the southern part of the ice shelf.

In areas of the ice shelf where there is little glacier inflow (e.g. Foyn Point and Cape Disappointment domains; Fig. 2) networks of interconnected meltwater streams dominate the surface drainage patterns. The drainage patterns of the streams suggest that the large glacier flanks (e.g. the north side of Crane outflow) and interglacier regions are lower in elevation than the central glacier outflow regions. Indeed, in the area of domains 1–3 (Fig. 2), where there are no longitudinal surface structures to indicate significant glacier inflow, networks of meltwater streams flow towards the ice-shelf front (Fig. 3a). Elevation maps of the ice-shelf surface from radar altimetry (Doake and others, 1998) concur with the suggestion of thinner shelf ice in the suture regions.

In February 2000 an extensive network of meltwater ponds and streams is visible on the ice-shelf surface (Fig. 4a and b). A drained meltwater pond (doline) is visible on the lower left of the image (labelled 1 in Fig. 4a; see also Bindschadler and others, 2002). Meltwater ponds and streams appear to follow the local topographic slope on the ice-shelf surface (upper part of image), but they also fill depressions on its surface along longitudinal surface structures (centre of image).

Meltwater-pond growth on the ice-shelf surface was rapid in the 25 day interval between the acquisitions of the two images. On 27 January 2000 there were 1381 individual meltwater ponds with a total surface area of 251 km^2 on the ice-shelf surface. By 21 February 2000 there were 2696 individual meltwater ponds with a total surface area of 365 km^2. In both cases, the majority of ponds were small (mean meltwater-pond area of 0.18 km^2 in January 2000 and 0.13 km^2 in February 2000). Large rifts were visible near the ice-shelf front (labelled 4 and 5 in Fig. 3b) as well as in the

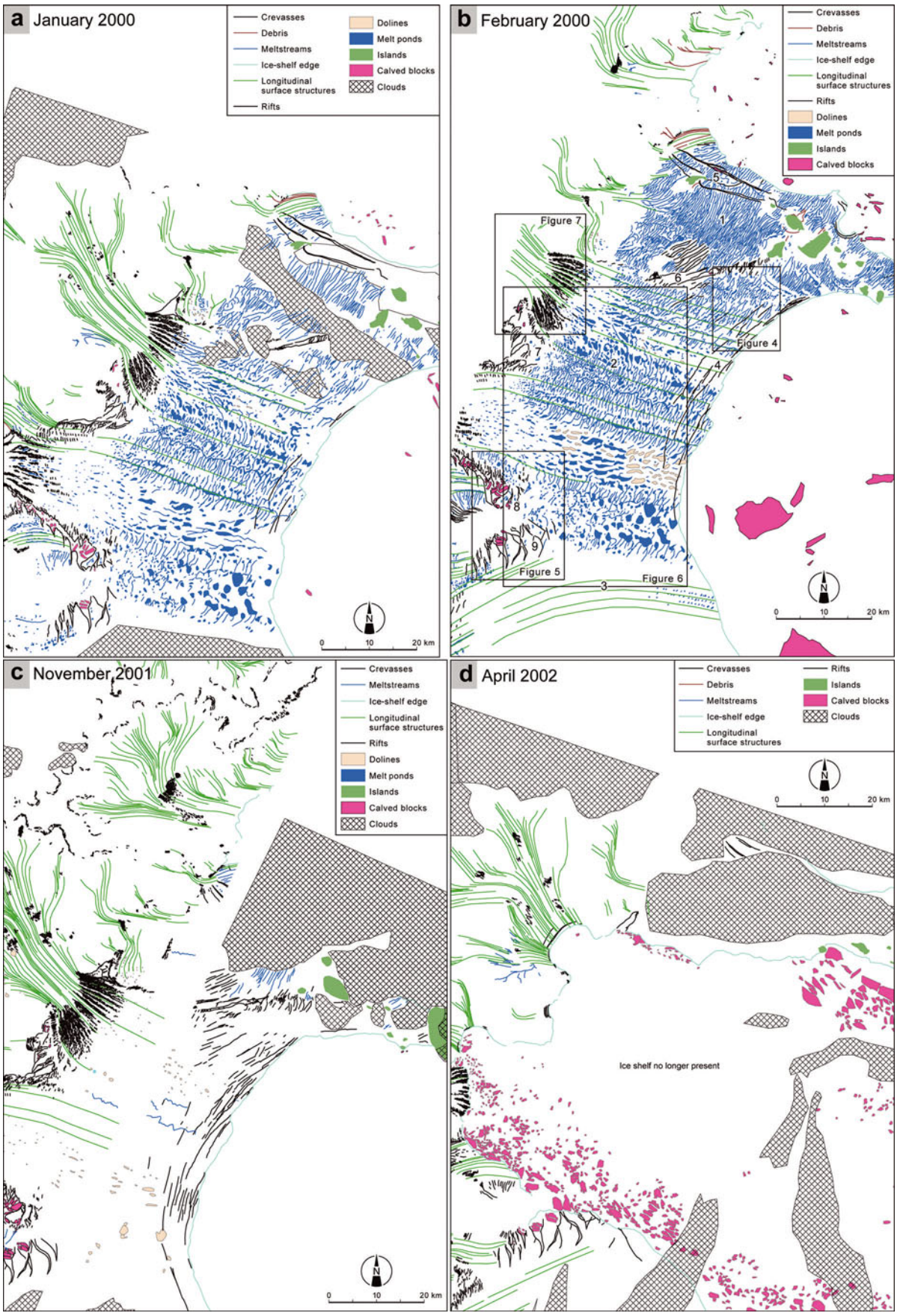

Fig. 3. Sequence illustrating the changes in surface structures on the Larsen B ice shelf between January 2000 and April 2002. (a) Structural interpretation from January 2000. (b) Structural interpretation from February 2000. Numbers 1–9 refer to features on the surface of the ice shelf discussed in the text. Boxes indicate the locations of other figures. (c) Structural interpretation from November 2001. (d) Structural interpretation from April 2002. Note that there is little change in the position of the ice-shelf edge between February 2000 and November 2001 but that the number of rifts and crevasses near the ice-shelf edge has increased by November 2001. By April 2002 the ice shelf has completely disappeared. Numbers refer to localities discussed in the text.

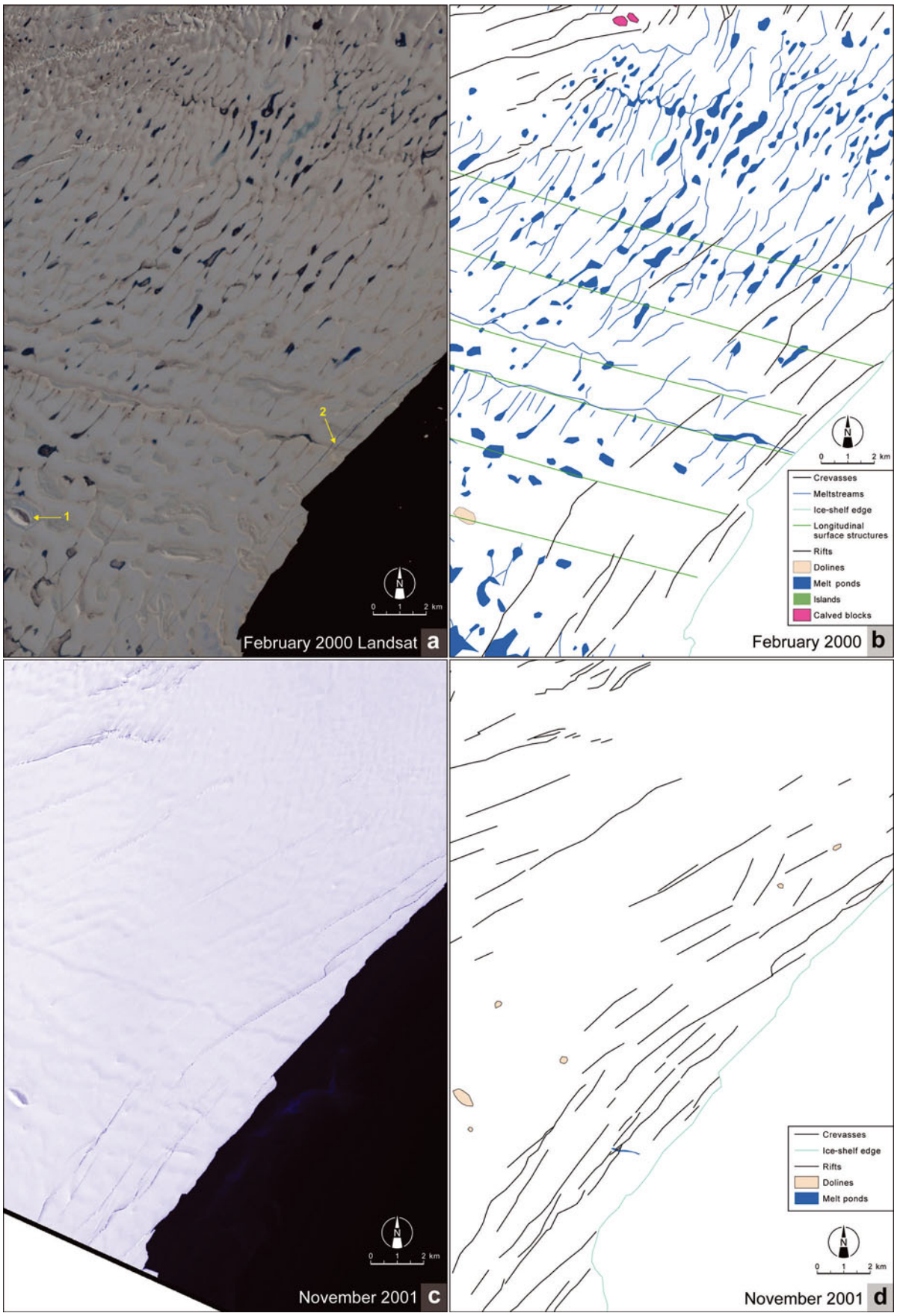

Fig. 4. Changes near the edge of the Larsen B ice shelf between February 2000 and November 2001. (a) Detail of Landsat image acquired in February 2000. Arrow 1 indicates doline; arrow 2 indicates rifts cutting through meltwater streams. (b) Interpretation of the same area. Note that close to the ice-shelf edge the crevasses and rifts are sub-parallel to the ice-shelf edge and cross-cut the meltwater streams and ponds. (c) Detail of ASTER image acquired in November 2001. (d) Interpretation of the same area. Note that there are more rifts close to the ice-shelf edge than in the comparable scene from February 2000.

ice-shelf interior (labelled 6 in Fig. 3b). Rift systems in the ice shelf in the zones where the Hektoria/Green/Evans glacier system, Jorum Glacier and Crane Glacier (labelled 7, 8 and 9 in Fig. 3b) enter the ice shelf are described in more detail below. Longitudinal surface structures originating in the Hektoria/Green/Evans glacier system, Jorum Glacier and Crane Glacier catchments can be traced across the ice shelf as far as its front.

Large-scale changes in the Larsen B ice shelf between January 2000 and April 2002

A comparison of satellite images from January 2000 (Fig. 3a) and February 2000 (Fig. 3b) with the November 2001 (Fig. 3c) and April 2002 (Fig. 3d) images provides a detailed record of large-scale changes in ice-shelf fracturing, and therefore the stress regime, leading up to its collapse.

Close to the ice-shelf front, crevasses and rifts are developed sub-parallel to the ice-shelf front. The crevasses and rifts cut through (cross-cut) the meltwater streams and ponds (labelled 2 in Fig. 4a). The number and length of rifts close to the ice-shelf front increased between February 2000 and November 2001 (Fig. 4c and d).

Changes in the tributary-glacier rift systems between February 2000 and April 2002

At several points along the grounding line of the ice shelf, major glacier domains are merged to form the ice shelf. However, these regions, typically near capes of rock on the coastline, are marked by major rifting, forming upstream of the capes on either side, and with rifts and melange (areas that consists of a mixture of dissimilar materials) downstream of the merge region of the glacier domains. Open water containing calved icebergs and brash ice is visible within the rifts (e.g. at points labelled 1 and 2 in Fig. 5a). These rift systems are present in all pre-ice-shelf collapse images of the Larsen B ice shelf (e.g. in February 2000 (Fig. 5a) and November 2001 (Fig. 5b)), and after ice-shelf collapse in April 2002 (Fig. 5c).

There were large tributary-glacier rift systems as far as ~40 km from the pre-collapse ice-shelf front. Rifts form in the less-active zones between active coalescing tributary glaciers (Fig. 3a–d). The largest rift systems are those at Foyn Point and Cape Disappointment (Fig. 5). Rift enlargement and the growth of new rifts is apparent in the interval between the January and February 2000 images and the November and December 2001 scenes. Mapping of the rifted 'blocks' shows that these blocks rotated significantly in the intervening time, by up to 45°, indicating non-steady behaviour and increased ice-shelf shearing in this region (Fig. 5a and b). Moreover, examination of the areas downstream of the suture regions indicates there are no downstream 'rift shadows'. This indicates that the rift patterns at Foyn Point and Cape Disappointment are relatively new features of the ice shelf and did not form, or at least formed much less frequently, in the past. Skvarca and others (1999) show a Landsat Thematic Mapper (TM) image from 1 March 1986, with just three rifts in the vicinity of Cape Disappointment, and none of the rifted melange we have mapped north of the cape was present at that time. Similarly, far less rifting is visible near Foyn Point in the 1986 Landsat TM image.

Image-to-image cross-correlation techniques (Scambos and others, 1992) were used to make ice-velocity measurements in the Foyn Point and Cape Disappointment regions (Fig. 6). In the Foyn Point region these measurements indicate ice-flow speeds of 460–525 m a^{-1} in the regions downstream of Foyn Point in the early 2000 to late 2001 interval (using the 21 February 2000 and 22 November 2001 image pair, a separation of 1.75 years). Rifts in this region decreased in extent and increased in spacing downstream of Foyn Point and are no longer discernible beyond ~10 km from Foyn Point. This suggests that the large rifts, and the separation of the shelf ice from the cape, began ~20–25 years ago. Similarly, at Cape Disappointment, measurements indicate large variations in ice-flow speeds between the ice shelf in the Cape Disappointment region and downstream of the Cape.

In the post-ice-shelf-collapse image acquired in April 2002 (Fig. 5c) it is clear that the ice-shelf front had receded as far back as these pre-existing rifts and these rift systems defined the maximum inland collapse position.

Changes in ice-shelf tributary glaciers between February 2000 and April 2002

The former tributary glaciers to the Larsen B ice shelf now form calving fronts in the Larsen embayment. The temporal transition from ice-shelf tributary glacier to calving glacier is exemplified by the Hektoria/Green/Evans glacier system. In February 2000, this glacier was one of the main tributaries of the former Larsen B ice shelf (Fig. 7a). Spreading crevasses indicate the onset of extensional flow at the point where the glacier enters the ice shelf. Longitudinal surface structures developed in the main trunk of Hektoria Glacier can be traced all the way to the ice-shelf front (Fig. 3a). Downglacier, there is an irregular surface topography composed of ridges and depressions inherited from the closed crevasses and longitudinal surface structures (Fig. 3a). Meltwater ponds occupy these surface depressions (Fig. 7a). There is little visible change between the situation in February 2000 and January 2001 (Fig. 7b). By April 2002, following the collapse of the Larsen B ice shelf, Hektoria Glacier formed a large calving front (Fig. 7c). Large transverse rifts and crevasses are visible in the glacier behind the newly formed calving front.

Upstream of the grounding line, crevasse changes indicate significant changes in the stress regime of the glacier in the aftermath of ice-shelf loss. This is particularly evident in Hektoria Glacier, the most rapidly accelerating glacier of the Larsen B ice shelf tributaries after the collapse. Comparison of pre-collapse images (Fig. 3a–c) with the post-collapse image (Fig. 3d) shows that in regions ~10 km upstream of the grounding line there was a rapid transition from shear-dominated crevasse styles (Fig. 3a–c) to widespread transverse fracturing indicative of much lower longitudinal back-stress (Fig. 3d). As noted by Rignot and others (2004) and Scambos and others (2004) this was associated with velocity acceleration of a factor of 5–8 in the 18 months following break-up and significant (tens of metres) ice surface lowering.

INTERPRETATION OF KEY STRUCTURES AND THEIR SIGNIFICANCE FOR ICE-SHELF COLLAPSE

Longitudinal surface structures

Longitudinal surface structures inherited from the tributary glaciers are the dominant flow-related feature on the surface of the ice shelves (Fig. 3a–c). This structure, also previously

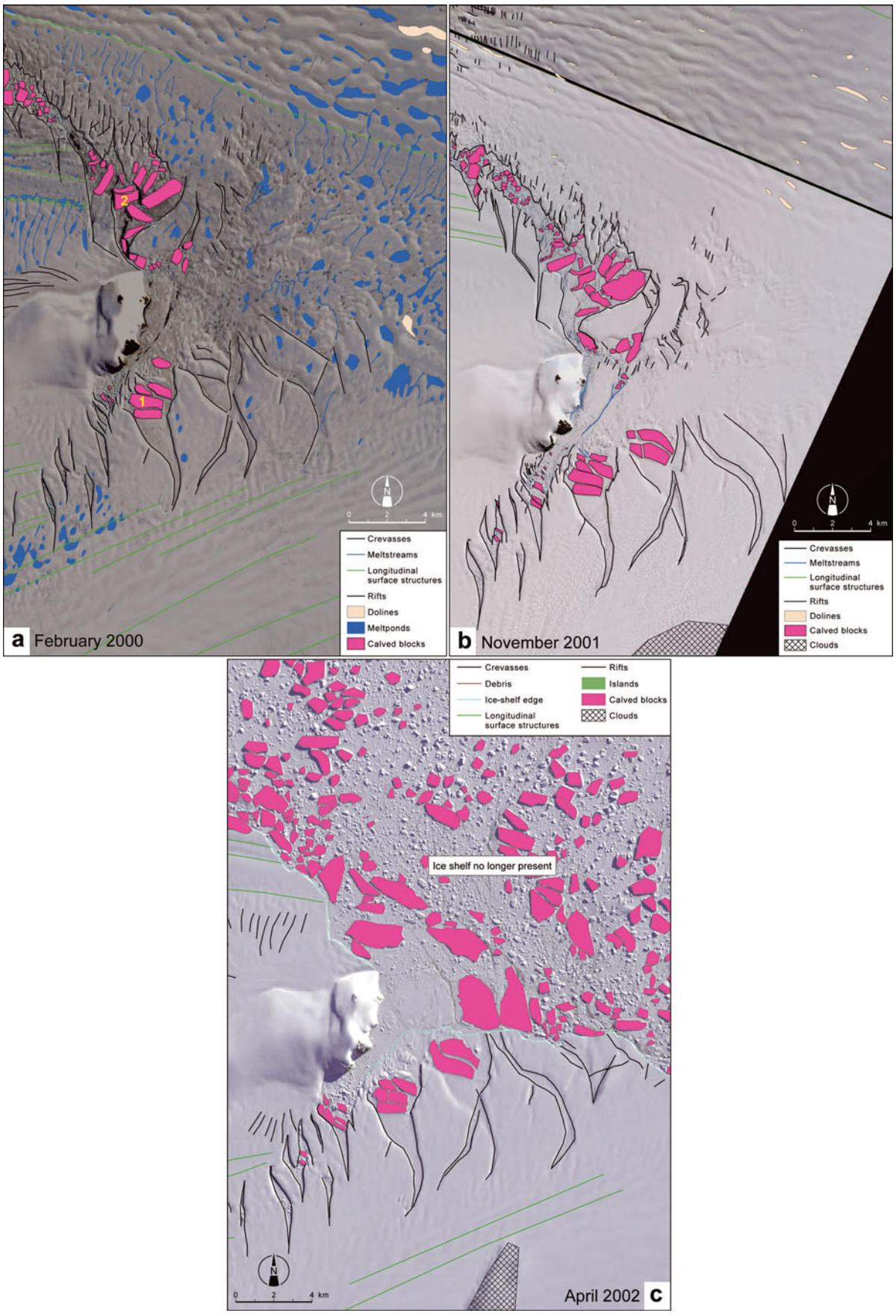

Fig. 5. (a, b) Detail of the southern part of Larsen B ice shelf prior to ice-shelf collapse in February 2000 (a) and November 2001 (b). (c) The situation after ice-shelf collapse in April 2002. Note that large rift systems containing open water and calved icebergs, labelled 1 and 2 in (a), existed prior to ice-shelf collapse. Note also the rotation of the blocks within the rifts around area 2 between February 2000 and November 2001. The rifts later formed the inward limit of ice-shelf collapse (c).

referred to as flow stripes, flowbands, flowlines or streak lines (Crabtree and Doake, 1980; Reynolds and Hambrey, 1988; Swithinbank and others, 1988; Casassa and Brecher, 1993; Fahnestock and others 2000), is developed parallel to the margins of individual flow units. On valley glaciers, where a three-dimensional relationship can be demonstrated, these longitudinal surface structures have been termed foliation (Hambrey and Glasser, 2003), but we have avoided this term because we cannot demonstrate that these structures are three-dimensional. One of the most striking attributes of these features is their persistence; in many cases, the longitudinal structures can be followed for ~100 km from their origin in tributary glaciers to the ice-shelf front. We infer that where these features are present, tributary glaciers are fast-flowing or active and that where they are absent tributary glaciers are less active.

The physical explanation for the origin of these longitudinal surface structures is unclear. Merry and Whillans (1993) considered that these features form in relation to localized high shear strain rates in ice streams near their onset areas. Another possibility is that they represent 'shear zones' within individual flow units. However, Casassa and Brecher (1993) found no velocity discontinuities across the boundaries between flow stripes on Byrd Glacier, which suggests that their persistence cannot be explained by lateral shear between the stripes. A more likely explanation is that these structures are created by the visco-plastic deformation or folding of pre-existing inhomogeneities, i.e. primary stratification, under laterally compressive and longitudinally tensile stresses (Hambrey, 1977; Hooke and Hudleston, 1978). The structures may be formed by this mechanism where ice flow interacts with a bedrock feature at some point upstream; shear and compressive forces create an inhomogeneity within the ice that persists for long distances in the absence of any downstream overprinting. Longitudinal surface structures are therefore common and long-lived on ice streams and fast-flowing glaciers where stress and bedrock interactions tend to be small. They are formed upstream as the glacier begins rapid flow and persist downstream because fast-flowing glaciers and ice streams have lower stresses. Further investigation of these features (e.g. using ice-penetrating radar to investigate their three-dimensional structure) is required to establish their precise origin.

Surface meltwater features (streams, ponds and dolines)

Meltwater features clearly indicate the presence of abundant ice-shelf surface melting in the years prior to ice-shelf collapse, an interpretation confirmed by nearby automatic weather station readings (Van den Broeke, 2005). The precise form and location of meltwater ponds and streams is closely related to glacier surface structures. For example, enclosed meltwater ponds form preferentially on the ice-shelf surface in the Crane Glacier domain because here the ice-shelf surface has a rough, pock marked surface inherited from upstream crevasses and longitudinal surface structures. On the Hektoria/Green/Evans glacier system domain (domain 5 in Fig. 2), where the ice-shelf surface is smoother, both surface meltwater ponds and streams exist (Fig. 3a and b). Thus the ice-shelf surface is dominated by many small ponds (1381 individual meltwater ponds with a total surface area of 251 km^2 in January 2000, and 2696 individual meltwater ponds with a total surface area of 365 km^2 in February 2000).

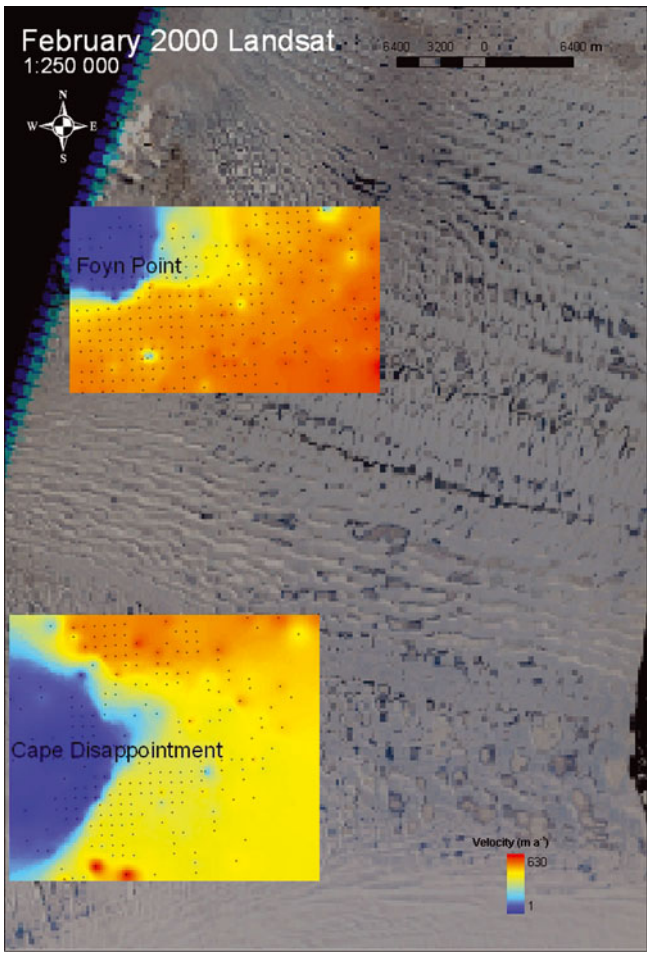

Fig. 6. Ice-velocity measurements in the Foyn Point and Cape Disappointment regions between 21 February 2000 and 22 November 2001 using image-to-image cross-correlation techniques (Scambos and others, 1992). Dots indicate ice-motion measurement vector midpoints from which the velocity fields were interpolated.

In other places, where longitudinal surface structures dominate and in regions of low ice input from upstream sources, meltwater ponds do not form and instead linear meltwater streams follow these structures (Fig. 3a and b). Long, linear meltwater streams also form close to the ice-shelf front where the ice-shelf surface slopes downward towards the ice-shelf front. Close to the ice-shelf front, crevasses and rifts cross-cut the meltwater streams and ponds (Fig. 4b). From this cross-cutting relationship, we infer that the fractures are younger than the meltwater features. Here there is no direct evidence that the fractures are being opened up by meltwater streams or by meltwater ponds draining into rifts and crevasses (MacAyeal and others, 2003), so, if this is occurring, it must be at a scale smaller than the resolution of the images used here. Instead, the rifts and crevasses appear to open up sub-parallel to the ice-shelf front under the influence of some other tensional regime, possibly related to extensional flow at the ice-shelf front.

Tributary-glacier rift systems

We suggest that the rifts opened up in these locations because of the strong lateral shear imparted on the less-active zones by the more-active flow units. These areas represent places where the ice shelf was in effect 'ripped'

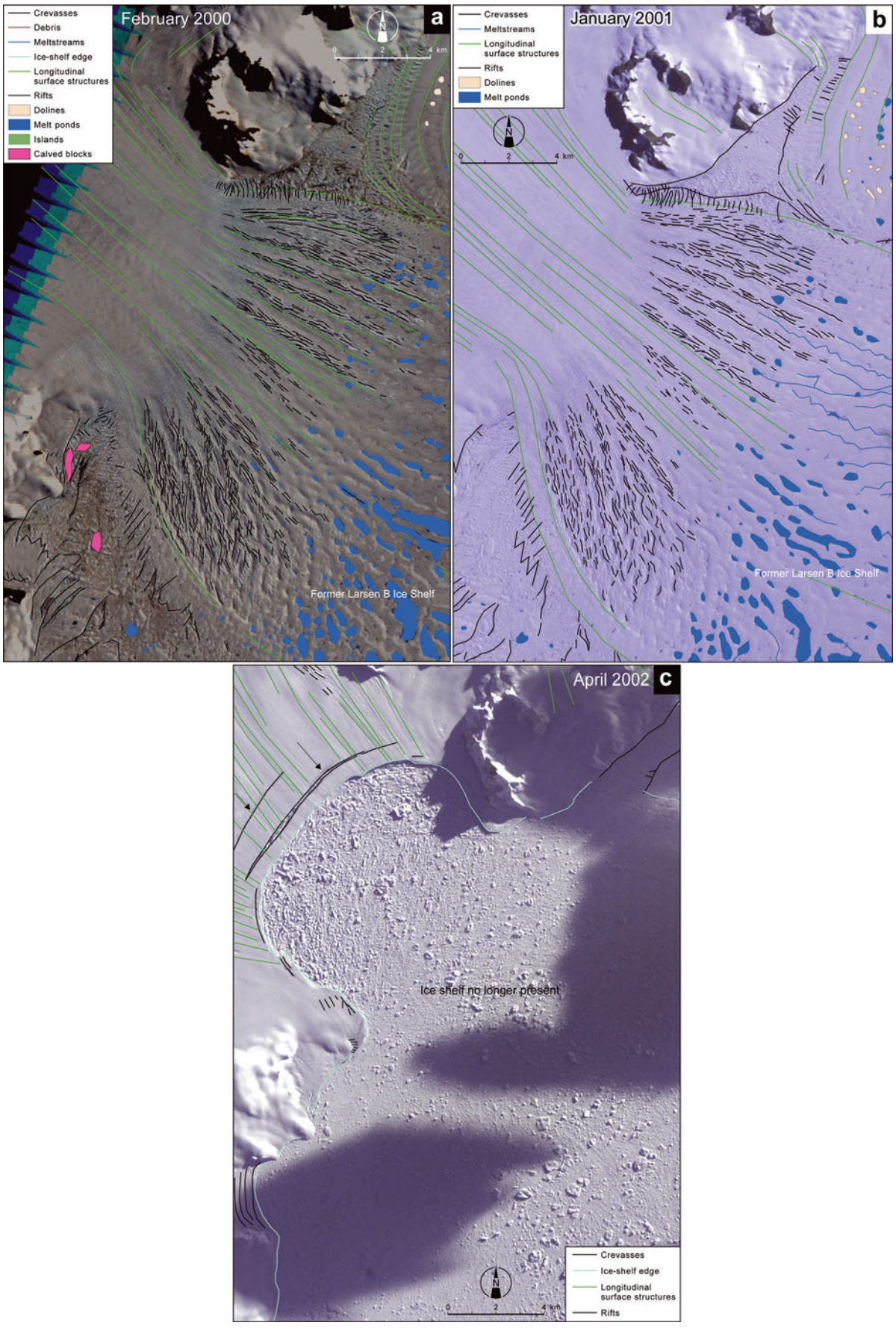

Fig. 7. The temporal transition from ice-shelf tributary to calving glacier at the Hektoria/Green/Evans glacier system. (a) Spreading crevasses at the point where the glacier entered the former Larsen B ice shelf in February 2000. (b) A similar pattern of spreading crevasses visible in January 2001. (c) 'New' calving front of the glacier in April 2002 after the collapse of the Larsen B ice shelf. Location of newly formed transverse crevasses and rifts behind the calving front are indicated by arrows.

open between the active flow units to either side. We do not know the precise composition or mechanical strength of the melange that occupies these rifts, but it appears to contain 'calved' icebergs, brash ice, refrozen surface meltwater, blown snow and marine water. The melange within these rifts is re-incorporated into the ice shelf as the rifts are advected down-ice by ice-shelf flow. From the open water and brash ice observed in the upstream-most parts of the inter-domain rifts, we infer that the ice shelf was relatively thin in these areas and unlikely to provide much mechanical strength to the shelf (cf. Jezek and Liu, 2005).

An important observation is the lack of downstream rift 'shadows' at both Foyn Point and Cape Disappointment. The absence of these downstream shadows indicates that these rifts are relatively new features of the ice shelf, formed within the last ~20 years. This is not the case on other ice shelves, for example the Ross or Ronne Ice Shelf where rift patterns can be traced down-ice for hundreds of kilometres, indicating centuries of steady behaviour (Fahnestock and others, 2000). When coupled with the ice velocity data, these rifts, and their absence downstream, suggest that the ice shelf began to change significantly ~20 years ago. This is consistent with the time when melt ponding began to become widespread across the ice-shelf surface (MacAyeal and others, 2003; Van den Broeke, 2005) and may correlate with thinning of the ice shelf due to warmer water infiltration (Williams and others, 2002; Shepherd and others, 2003; Payne and others, 2004).

The evidence of relatively recent development of the tributary rift systems from the imagery suggests that the sutures were weakened significantly in the years leading up to the collapse in 2002. Thus the incremental loss of ice-shelf front may be enough to increase susceptibility to break-up because the loss of ice-shelf front causes increased shear and decoupling of the upstream suture areas with the coast.

Ice-shelf front rifts

Rifts close to the ice-shelf front, such as those shown in Figure 4, propagate as the ice shelf flexes because of ice-shelf deformation during horizontal motion (Rist and others, 2002; Larour and others, 2004). They are important because rift spacing strongly influences the dimensions of icebergs, as well as the frequency and magnitude of iceberg-calving events (Weiss, 2004).

Ice-shelf tributary domains

Tributary-glacier domains on the ice-shelf surface are marked by the longitudinal surface structures visible within individual tributary-glacier flow units. Longitudinal surface structures originating in the trunks of these glaciers can be traced, uninterrupted, all the way to the ice-shelf front, implying that these glaciers are fast-flowing and actively contribute mass to the ice shelf. Splaying crevasse patterns and bowed longitudinal surface structures also indicate that there is divergence of flow as these glaciers enter the ice shelf (Fig. 2). Between the active domains are domains lacking significant up-glacier catchments and without longitudinal surface structures, inferred to represent slower-flowing or less-active flow units. The structural evidence agrees with earlier field- and satellite-derived velocity and longitudinal strain-rate measurements, which have established that individual flow units on the former Larsen B ice shelf had markedly different velocity, longitudinal strain rates and rheology (e.g. Bindschadler and others, 1994; Skvarca and others, 1999; Rack and Rott, 2004; Vieli and others, 2006, 2007; Khazendar and others, 2007).

Our velocity measurements (Fig. 6) and the presence of open-rift systems in the zones between the more-active and less-active flow units around Foyn Point and Cape Disappointment support the interpretation that velocity and longitudinal strain rates differ between flow units. We suggest that the rifts formed in these locations because of the strong lateral shear imparted on the less-active zones by the more-active flow units.

Finally, we note that by far the largest contribution to the ice shelf comes from only four tributary glaciers: the Hektoria/Green/Evans glacier system (domain 5 in Fig. 2), Punchbowl Glacier (domain 7 in Fig. 2), Jorum Glacier (domain 8 in Fig. 2) and Crane Glacier (domain 10 in Fig. 2).

Changes in ice-shelf tributary glaciers between February 2000 and April 2002

Following the collapse of the Larsen B ice shelf, former tributary glaciers such as Hektoria/Green/Evans, Jorum and Crane glaciers now form large calving fronts in the Larsen embayment (Fig. 7c). Large transverse rifts and crevasses in these glaciers behind the newly formed calving front indicate longitudinal extension. This type of extension is compatible with the finding that tributary glaciers have thinned and accelerated considerably since ice-shelf collapse (Thomas and others, 1979; Van der Veen, 1996; Rignot and others, 2004; Scambos and others, 2004). The presence of an ice shelf provides back-stress or decreases the magnitude of the extensional stress near the grounding line and therefore inhibits glacier motion behind the ice shelf (Dupont and Alley, 2005). Once this buttressing effect is removed, the tributary glaciers are free to accelerate. The volume of calved icebergs immediately in front of the glacier indicates that calving is an active and ongoing process.

DISCUSSION

Ice-shelf collapse: structural precursors

We have defined domains on the Larsen B ice shelf related to glacier-source areas (Fig. 2) and have demonstrated that, prior to collapse, the largest contribution to the ice shelf came from only four tributary glaciers: the Hektoria/Green/Evans glacier system, Punchbowl Glacier, Jorum Glacier and Crane Glacier. Between these glacier-fed active flow units were less-active flow units. The active flow units were sutured downstream. In recent years, thinning of the ice shelf, and, just prior to collapse, loss of the ice-front region of the ice shelf, led to a much weaker shelf, prone to extension and fracturing.

Unless the upstream regions of sutures between individual flow units were strong, which we consider unlikely, these structural discontinuities would have rendered the ice shelf mechanically weak, and therefore prone to disintegration, prior to its collapse. Failures developed along the flow-unit boundaries, which were only weakly sutured, so ice-shelf collapse proceeded rapidly along these lines of structural weakness. The decoupling of the suture regions from the coast around Foyn Point and Cape Disappointment is a potential indicator of impending ice-shelf break-up. On the existing Larsen C ice shelf we note that tributary suture regions do not, at present, show the rifting and melange that we observed in the pre-collapse Larsen B. This would

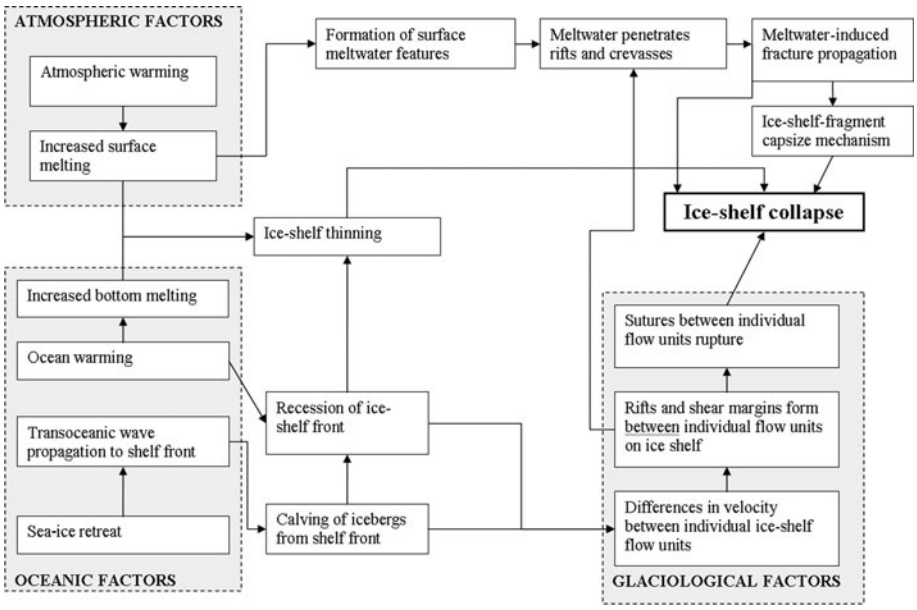

Fig. 8. Flow diagram showing factors influencing ice-shelf collapse. Items within shaded areas represent causal factors. See text for full discussion.

indicate that the Larsen C ice shelf is probably not in immediate danger of collapse. There is, however, some indication of new 'tributary junction' rifting in the remnant Larsen B ice shelf, which may indicate a potential for further recession of that ice shelf.

Ice-shelf susceptibility to break-up was also increased by mass loss at the ice-shelf front because the loss of ice at the shelf front removed the strongest portions of the shelf, i.e. the most sutured, bonded and thickened (by accumulation) portions in the inter-domain regions. An important observation of ice-shelf disintegration is that it occurred through the formation of many narrow, needle-shaped icebergs instead of the large tabular icebergs that characterized pre-collapse iceberg calving. The structural features that we have observed (e.g. the very long, closely spaced rifts and crevasses) mirror the size of many of the icebergs formed during disintegration and therefore help to explain the dramatic change in the size distribution of Larsen B ice shelf icebergs before and during collapse.

Even if our assertion that the Larsen B ice shelf was mechanically weak prior to its collapse is correct, a trigger is still required for its sudden and rapid disintegration. The leading hypothesis for this rapid disintegration is that of Scambos and others (2000) and MacAyeal and others (2003), who proposed that ponded meltwater on the ice-shelf surface acted as a mechanical force in the crevasses, causing breaks in the ice shelf and thus accelerating ice-shelf disintegration. However, another hypothesis emerges from our structural analysis. This is the possibility that ice-shelf collapse may have been initiated along structural lines, either by ice-shelf acceleration or by perturbations in the input velocity from one or more of the tributary-glacier flow units. A rapid or sustained period of acceleration or deceleration of one of these tributary glaciers or change in the longitudinal stress regime would be sufficient to cause the suture between flow units to rupture (especially in a climatically thinned ice shelf; cf. Vieli and others, 2007) and thus cause the ice shelf to disintegrate along pre-existing lines of structural weakness.

There is independent evidence to support this hypothesis from three sources. First are pre-collapse stake measurements on the former Larsen B ice shelf, which show disturbances in mass balance and ice-flow behaviour in the years prior to collapse (Rack and others, 2000). Second are satellite-derived ice-shelf velocities that clearly show pre-collapse velocity differentials between individual ice-shelf tributary glaciers for the adjacent Larsen A ice shelf (Bindschadler and others, 1994). Third are the satellite observations and modelling experiments of Vieli and others (2007) that indicate the ice shelf was undergoing a significant acceleration before its collapse in 2002.

We suggest that a number of atmospheric, oceanic and glaciological factors contribute to ice-shelf collapse (Fig. 8). Rapid ice-shelf disintegration is aided by structural factors, as well as the large quantities of surface meltwater observed on the ice shelf in 2002 (MacAyeal and others, 2003; Van den Broeke, 2005). A related possibility is that changes in velocity structure were initiated by external factors such as ocean warming (Williams and others, 2002; Shepherd and others, 2003; Payne and others, 2004) or transoceanic wave propagation (MacAyeal and others, 2006). It is probably not possible to ascribe ice-shelf collapse singularly to one of these factors. It is therefore possible that in 2002 the Larsen B ice shelf simply crossed an environmental threshold where the interplay between atmospheric factors (e.g. increased surface melting and associated ice-shelf thinning), oceanic factors (e.g. increased bottom melting and associated ice-shelf thinning and recession, as well as the potential for increased iceberg calving) and glaciological factors (e.g. differences in upstream surface mass balance and velocity between flow units, and structural weaknesses) was sufficient to cause an irreversible decline.

CONCLUSIONS

In this study we have provided a detailed structural glaciological analysis of the changes in surface structures on the Larsen B ice shelf from a series of visible-channel

satellite images acquired between January 2000 and April 2002 and the RADARSAT-1 Antarctic Mapping Project (RAMP) mosaic of 1997. Mapped structures include longitudinal surface structures, rifts, crevasses, meltwater streams, meltwater ponds and dolines. Longitudinal surface structures are particularly important on the Larsen B ice shelf because they can be used to define individual tributary-glacier flow units (domains) and their contribution to the pre-collapse ice shelf. Using these data, we draw the following conclusions:

1. The former Larsen B ice shelf consisted of four sutured flow units fed by Crane Glacier, Jorum Glacier, Punchbowl Glacier and the Hektoria/Green/Evans glacier system. Between these active glacier-fed flow units were 'suture zones' of thinner ice where the feeder glaciers merged to form the shelf.
2. Prior to collapse, large open-rift systems (with floating brash ice) were present offshore of Foyn Point and Cape Disappointment. In the years just preceding break-up, these rifts became more pronounced and ice blocks in the rifts rotated because of the strong lateral shear in the zone separating active and less-active flow units. Velocity mapping of the suture regions indicates that the major rifts are a recent feature of the ice shelf, and were not present over ~20 years ago.
3. The geographical extent of the ice-shelf collapse was controlled partly by the location of these large open-rift systems offshore of Foyn Point and Cape Disappointment. When the ice shelf collapsed, disintegration proceeded as far back as these rifts.
4. A number of factors (atmospheric, oceanic and glaciological) combined to contribute to the rapid demise of the Larsen B ice shelf in 2002. We suggest that structural glaciological discontinuities played a large part because they rendered the ice shelf mechanically weak prior to its collapse. Failures along weakly sutured flow-unit boundaries were particularly important. Loss of ice at the shelf front may also have played a role because this process removed the strongest portions of the shelf, i.e. the most sutured and bonded portions in the inter-domain regions.
5. Ice-shelf collapse may have been initiated by perturbations in the input velocity from one or more of the tributary-glacier flow units, which caused the sutures between flow units to rupture and thus caused the ice shelf to disintegrate rapidly.

ACKNOWLEDGEMENTS

N.F. Glasser acknowledges support from the US–UK Fulbright Commission as a Fulbright Distinguished Scholar at the US National Snow and Ice Data Center in 2007 and from a CIRES (Cooperative Institute for Research in Environmental Sciences) Research Fellowship. D. Quincey helped with the production of Figure 6. We acknowledge constructive reviews from J. Bassis and D. Vaughan. T. Scambos acknowledges support from NASA grant NNG06GA69G.

REFERENCES

Bindschadler, R.A., M.A. Fahnestock, P. Skvarca and T.A. Scambos. 1994. Surface-velocity field of the northern Larsen Ice Shelf, Antarctica. *Ann. Glaciol.,* **20**, 319–326.

Bindschadler, R., T. Scambos, H. Rott, P. Skvarca and P. Vornberger. 2002. Ice dolines on Larsen Ice Shelf, Antarctica. *Ann. Glaciol.,* **34**, 283–290.

Casassa, G. and H.H. Brecher. 1993. Relief and decay of flow stripes on Byrd Glacier, Antarctica. *Ann. Glaciol.,* **17**, 255–261.

Crabtree, R.D. and C.S.M. Doake. 1980. Flow lines on Antarctic ice shelves. *Polar Rec.,* **20**(124), 31–37.

De Angelis, H. and P. Skvarca. 2003. Glacier surge after ice shelf collapse. *Science,* **299**(5612), 1560–1562.

Domack, E. *and 9 others*. 2005. Stability of the Larsen B ice shelf on the Antarctic Peninsula during the Holocene epoch. *Nature,* **436**(7051), 681–685.

Dupont, T.K. and R.B. Alley. 2005. Assessment of the importance of ice-shelf buttressing to ice-sheet flow. *Geophys. Res. Lett.,* **32**(4), L04503. (10.1029/2004GL022024.)

Evans, J. and C. Ó Cofaigh. 2003. Supraglacial debris along the front of the Larsen-A Ice Shelf, Antarctic Peninsula. *Antarct. Sci.,* **15**(4), 503–506.

Evans, J. and C.J. Pudsey. 2002. Sedimentation associated with Antarctic Peninsula ice shelves: implications for palaeoenvironmental reconstructions of glacimarine sediments. *J. Geol. Soc. London,* **159**(3), 233–237.

Fahnestock, M.A., T.A. Scambos, R.A. Bindschadler and G. Kvaran. 2000. A millennium of variable ice flow recorded by the Ross Ice Shelf, Antarctica. *J. Glaciol.,* **46**(155), 652–664.

Glasser, N., B. Goodsell, L. Copland and W. Lawson. 2006. Debris characteristics and ice-shelf dynamics in the ablation region of the McMurdo Ice Shelf, Antarctica. *J. Glaciol.,* **52**(177), 223–234.

Hambrey, M.J. 1977. Foliation, minor folds and strain in glacier ice. *Tectonophysics,* **39**(1–3), 397–416.

Hambrey, M.J. and J.A. Dowdeswell. 1994. Flow regime of the Lambert Glacier–Amery Ice Shelf system, Antarctica: structural evidence from Landsat imagery. *Ann. Glaciol.,* **20**, 401–406.

Hambrey, M.J. and N.F. Glasser. 2003. The role of folding and foliation development in the genesis of medial moraines: examples from Svalbard glaciers. *J. Geol.,* **111**(4), 471–485.

Hjort, C., M.J. Bentley and Ó. Ingólfsson. 2001. Holocene and pre-Holocene temporary disappearance of the George VI Ice Shelf, Antarctic Peninsula. *Antarct. Sci.,* **13**(3), 296–301.

Hooke, R.Le B. and P.J. Hudleston. 1978. Origin of foliation in glaciers. *J. Glaciol.,* **20**(83), 285–299.

Hulbe, C.L., D.R. MacAyeal, G.H. Denton, J. Kleman and T.V. Lowell. 2004. Catastrophic ice shelf breakup as the source of Heinrich event icebergs. *Paleoceanography,* **19**(1), PA1004. (10.1029/2003PA000890.)

Jezek, K.C. and H.X. Liu. 2005. Structure of southeastern Antarctic Peninsula ice shelves and ice tongues from synthetic aperture radar imagery. *J. Glaciol.,* **51**(174), 373–376.

Joughin, I. and L. Padman. 2003. Melting and freezing beneath Filchner–Ronne Ice Shelf, Antarctica. *Geophys. Res. Lett.,* **30**(9), 1477–1480.

Khazendar, A., E. Rignot and E. Larour. 2007. Larsen B Ice Shelf rheology preceding its disintegration inferred by a control method. *Geophys. Res. Lett.,* **34**(19), L19503. (10.1029/2007GL030980.)

Larour, E., E. Rignot and D. Aubry. 2004. Processes involved in the propagation of rifts near Hemmen Ice Rise, Ronne Ice Shelf, Antarctica. *J. Glaciol.,* **50**(170), 329–341.

MacAyeal, D.R., T.A. Scambos, C.L. Hulbe and M.A. Fahnestock. 2003. Catastrophic ice-shelf break-up by an ice-shelf-fragment-capsize mechanism. *J. Glaciol.,* **49**(164), 22–36.

MacAyeal, D.R. *and 13 others*. 2006. Transoceanic wave propagation links iceberg calving margins of Antarctica with storms in tropics and Northern Hemisphere. *Geophys. Res. Lett.,* **33**(17), L17502. (10.1029/2006GL027235.)

Merry, C.J. and I.M. Whillans. 1993. Ice-flow features on Ice Stream B, Antarctica, revealed by SPOT HRV imagery. *J. Glaciol.,* **39**(133), 515–527.

Morris, E.M. and D.G. Vaughan. 2003. Spatial and temporal variation of surface temperature on the Antarctic peninsula and the limit of viability of ice shelves. *In* Domack, E., A. Leventer, A. Burnett, R.A. Bindschadler, P. Convey and M. Kirby, *eds. Antarctic Peninsula climate variability – historical and paleoenvironmental perspectives*. Washington, DC, American Geophysical Union, 61–68. (Antarctic Research Series 79.)

Payne, A.J., A. Vieli, A. Shepherd, D.J. Wingham and E. Rignot. 2004. Recent dramatic thinning of largest West Antarctic ice stream triggered by oceans. *Geophys. Res. Lett.,* **31**(23), L23401. (10.1029/2004GL021284.)

Pritchard, H.D. and D.G. Vaughan. 2007. Widespread acceleration of tidewater glaciers on the Antarctic Peninsula. *J. Geophys. Res.*, **112**(F3), F03529. (10.1029/2006JF000597.)

Pudsey, C.J. and J. Evans. 2001. First survey of Antarctic sub–ice shelf sediments reveals mid-Holocene ice shelf retreat. *Geology,* **29**(9), 787–790.

Rack, W. and H. Rott. 2004. Pattern of retreat and disintegration of the Larsen B ice shelf, Antarctic Peninsula. *Ann. Glaciol.,* **39**, 505–510.

Rack, W., C.S.M. Doake, H. Rott, A. Siegel and P. Skvarca. 2000. Interferometric analysis of the deformation pattern of the northern Larsen Ice Shelf, Antarctic Peninsula, compared to field measurements and numerical modeling. *Ann. Glaciol.,* **31**, 205–210.

Reynolds, J.M. and M.J. Hambrey. 1988. The structural glaciology of George VI Ice Shelf, Antarctic Peninsula. *Br. Antarct. Surv. Bull.,* **79**, 79–95.

Rignot, E., G. Casassa, P. Gogineni, W. Krabill, A. Rivera and R. Thomas. 2004. Accelerated ice discharge from the Antarctic Peninsula following the collapse of Larsen B ice shelf. *Geophys. Res. Lett.,* **31**(18), L18401. (10.1029/2004GL020697.)

Rignot, E. *and 9 others*. 2005. Recent ice loss from the Fleming and other glaciers, Wordie Bay, West Antarctic Peninsula. *Geophys. Res. Lett.,* **32**(7), L07502. (10.1029/2004GL021947.)

Rist, M.A., P.R. Sammonds, H. Oerter and C.S.M. Doake. 2002. Fracture of Antarctic shelf ice. *J. Geophys. Res.,* **107**(B1). (10.1029/2000JB000058.)

Rott, H., P. Skvarca and T. Nagler. 1996. Rapid collapse of northern Larsen Ice Shelf, Antarctica. *Science,* **271**(5250), 788–792.

Rott, H., W. Rack, T. Nagler and P. Skvarca. 1998. Climatically induced retreat and collapse of northern Larsen Ice Shelf, Antarctic Peninsula. *Ann. Glaciol.,* **27**, 86–92.

Rott, H., W. Rack, P. Skvarca and H. De Angelis. 2002. Northern Larsen Ice Shelf, Antarctica: further retreat after collapse. *Ann. Glaciol.,* **34**, 277–282.

Scambos, T.A., M.J. Dutkiewicz, J.C. Wilson and R.A. Bindschadler. 1992. Application of image cross-correlation to the measurement of glacier velocity using satellite image data. *Remote Sens. Environ.,* **42**(3), 177–186.

Scambos, T.A., C. Hulbe, M. Fahnestock and J. Bohlander. 2000. The link between climate warming and break-up of ice shelves in the Antarctic Peninsula. *J. Glaciol.,* **46**(154), 516–530.

Scambos, T., C. Hulbe and M. Fahnestock. 2003. Climate-induced ice shelf disintegration in the Antarctic Peninsula. *In* Domack, E.W., A. Burnett, A. Leventer, P. Conley, M. Kirby and R. Bindschadler, *eds. Antarctic Peninsula climate variability: a historical and paleoenvironmental perspective*. Washington, DC, American Geophysical Union, 79–92. (Antarctic Research Series 79.)

Scambos, T.A., J.A. Bohlander, C.A. Shuman and P. Skvarca. 2004. Glacier acceleration and thinning after ice shelf collapse in the Larsen B embayment, Antarctica. *Geophys. Res. Lett.,* **31**(18), L18402. (10.1029/2004GL020670.)

Shepherd, A., D. Wingham, T. Payne and P. Skvarca. 2003. Larsen ice shelf has progressively thinned. *Science,* **302**(5646), 856–859.

Skvarca, P. 1994. Changes and surface features of the Larsen Ice Shelf, Antarctica, derived from Landsat and Kosmos mosaics. *Ann. Glaciol.,* **20**, 6–12.

Skvarca, P., W. Rack and H. Rott. 1999. 34 year satellite time series to monitor characteristics, extent and dynamics of Larsen B Ice Shelf, Antarctic Peninsula. *Ann. Glaciol.,* **29**, 255–260.

Swithinbank, C., K. Brunk and J. Sievers. 1988. A glaciological map of Filchner–Ronne Ice Shelf, Antarctica. *Ann. Glaciol.,* **11**, 150–155.

Thomas, R.H., T.J.O. Sanderson and K.E. Rose. 1979. Effect of climatic warming on the West Antarctic ice sheet. *Nature,* **277**(5695), 355–358.

Van den Broeke, M. 2005. Strong surface melting preceded collapse of Antarctic Peninsula ice shelf. *Geophys. Res. Lett.,* **32**(12), L12815 (10.1029/2005GL023247.).

Van der Veen, C.J. 1996. Tidewater calving. *J. Glaciol.,* **42**(141), 375–385.

Van der Veen, C.J. 2007. Fracture propagation as means of rapidly transferring surface meltwater to the base of glaciers. *Geophys. Res. Lett.,* **34**(1), L01501. (10.1029/2006GL028385.)

Vaughan, D.G. and C.S.M. Doake. 1996. Recent atmospheric warming and retreat of ice shelves on the Antarctic Peninsula. *Nature,* **379**(6563), 328–331.

Vieli, A., A.J. Payne, Z. Du and A. Shepherd. 2006. Numerical modelling and data assimilation of the Larsen B ice shelf, Antarctic Peninsula. *Philos. Trans. R. Soc. London, Ser. A,* **364**(1844), 1815–1839.

Vieli, A., A.J. Payne, A. Shepherd and Z. Du. 2007. Causes of pre-collapse changes of the Larsen B ice shelf: numerical modelling and assimilation of satellite observations. *Earth Planet. Sci. Lett.,* **259**(3-4), 297–306.

Weiss, J. 2004. Subcritical crack propagation as a mechanism of crevasse formation and iceberg calving. *J. Glaciol.,* **50**(168), 109–115.

Williams, M.J.M., K. Grosfeld, R.C. Warner, R. Gerdes and J. Determann. 2001. Ocean circulation and ice–ocean interaction beneath the Amery Ice Shelf, Antarctica. *J. Geophys. Res.,* **106**(C10), 22,383–22,399.

Williams, M.J.M., R.C. Warner and W.F. Budd. 2002. Sensitivity of the Amery Ice Shelf, Antarctica, to changes in the climate of the Southern Ocean. *J. Climate,* **15**(19), 2740–2757.

MS received 5 September 2007 and accepted in revised form 25 November 2007